Acta Cryst. (1994). B**50**, 86–96

Molecular and Electronic Structures of Two (Anticonvulsant) Diphenylhydantoin Derivatives

BY M. CIECHANOWICZ-RUTKOWSKA

Regional Laboratory of Physicochemical Analysis and Structural Research, Jagiellonian University, Ingardena 3, 30-060 *Kraków, Poland*

K. KIEĆ-KONONOWICZ

Department of Pharmaceutical Chemistry, Medical Academy, Skaleczna 10, 31-065 *Kraków, Poland*

AND S. T. HOWARD, H. LIEBERMAN AND M. B. HURSTHOUSE

*Department of Chemistry, University of Wales College of Cardiff, Cardiff CF*1 3*TB, Wales*

(*Received* 2 *December* 1992; *accepted* 26 *July* 1993)

Abstract

1-Benzyl-5,5-diphenyl-2,4-dioxo-3-imidazolidineacetic acid (AC), M_r = 400.434, triclinic, $P\bar{1}$, a = 8.7640 (3), b = 11.112 (1), c = 11.323 (2) Å, α = 102.10 (2), β = 95.44 (5), γ = 109.12 (1)°, V = 1002.65 (30) Å^3, Z = 2, D_x = 1.33 g cm^{-3}, $F(000)$ = 420, μ(Mo $K\alpha$) = 0.852 cm^{-1}, T = 293 K, R = 0.066 for 5551 unique observed reflections. The compound crystallizes from ethanol at room temperature in the form of colourless prisms. 3-(2,4-Dichlorobenzyl)-5,5-diphenyl-2,4-dioxo-1-imidazolidineacetic acid (AD), M_r = 469.323, monoclinic, $P2_1$, a = 8.0399 (7), b = 9.7237 (6), c = 26.9768 (12) Å, β = 94.281 (4)°, V = 2102.92 (96) Å^3, Z = 4, D_x = 1.48 g cm^{-3}, $F(000)$ = 968, μ(Mo $K\alpha$) = 3.417 cm^{-1}, T = 293 K, R = 0.066 for 5677 unique observed reflections. The compound crystallizes from ethanol at room temperature in the form of colourless prisms. Two approaches are employed in trying to understand the known differences in pharmacological activity: an analysis of the molecular geometries, and electronic structure calculations. A detailed analysis is made of the molecular geometries both from the X-ray diffraction results, and following energy minimization with molecular mechanics. The *ab initio* calculations employ the energy-minimized conformations. Several electronic properties are intercompared for AC, AD and their common parent molecule diphenylhydantoin (DPH). The analyses of geometry and electronic structure indicate dissimilarities between active and inactive compounds which may be linked to differences in the activity.

Introduction

In a search for new compounds with anticonvulsant properties, a series of DPH derivatives [(I) and (II)] were synthesized (Zejc *et al.*, 1989).

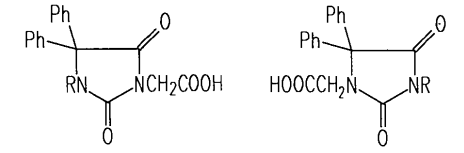

(I) (II)

AC (I, R = $PhCH_2$)
AD (II, R = $CH_2C_6H_3Cl_2$-2,4)

The aim was to determine the effect on the pharmacological activity of the compounds of a hydrogen-donating group at position 1 or 3 of the hydantoin ring, with a simultaneous substitution at the second N atom of the ring. Preliminary tests have shown that the most active 3-(2,4-dichlorobenzyl)-5,5-diphenyl-2,4-dioxo-1-imidazolidineacetic acid (AD) has antidepressant action but has no anticonvulsant properties, while 1-benzyl-5,5-diphenyl-2,4-dioxo-3-imidazolidineacetic acid (AC) has a protective action against pentetrazole-induced clonic tonic seizures (MET tests) (Zejc *et al.*, 1989; Kieć-Kononowicz, Zejc & Kolasa, 1989). It was found that chlorine substitution in the benzyl substituent group of AD did not change the activity, and since it produced better quality crystals it was used for X-ray structural analysis.

The X-ray structural study was undertaken with two aims in mind. Firstly, an analysis of the molecular geometry of the compounds AD and AC along the lines of earlier studies by Camerman & Camerman (1974) and Wong, Defina & Andrews (1986) might explain the pharmacological activity. These studies involved compounds (including DPH) active against maximal electroshock (MES). In fact, AC is active in MET tests; this could suggest that the mechanism of action is different with respect to DPH (Brouillette, Brown, Delorey & Liang, 1990), possibly because the former could interact with the benzodiazepine receptor. However, binding experiments carried out on rat brain membranes showed

that AC is scarcely active at this receptor (Borea, 1991). In view of the chemical similarity between AC and DPH, it seems reasonable that aspects of the model for active MES anticonvulsants might be relevant to the activity of AC.

Secondly, the possibility of an electronic basis for the activity differences might be explored with molecular orbital (MO) calculations. Such calculations have been applied to anticonvulsant drug compounds before, mostly at the semi-empirical level (Andrews, 1969; Aldrich & Kier, 1974; Andrews & Wong, 1989). More recently it has become feasible to carry out non-empirical calculations on compounds of this size, within the restrictions of small or minimal basis sets. Here we choose to concentrate on the electron density $\rho(\mathbf{r})$ and properties derived from it ('one-electron properties'), rather than attempt to analyze the (non-unique) one-electron wavefunctions (MO's). Recent advances in representing both theoretical and experimental electron densities (Jeffrey & Piniella, 1991) have provided a number of sensitive 'probes' which should prove useful in quantum pharmacology - these include distributed multipole analysis (DMA) (Stone, 1981); critical-point (CP) analysis (Bader, 1990); the Laplacian of the electron density, $\nabla^2\rho$; and various types of deformation density (DD) (Ruedenberg & Schwarz, 1990). This is in addition to more traditional indicators of electronic structure and reactivity, such as the electrostatic potential (Scrocco & Tomasi, 1978).

Experimental

X-ray measurements were made using an Enraf–Nonius FAST area detector and graphite-monochromated Mo $K\alpha$ radiation. With a detector-to-crystal setting (= DET) of 40 mm and a swing angle (θ) of -18°, reflections were found in two 5° ω-rotation regions separated by 90°. Orientation matrix and unit-cell dimensions were determined *via* the *INDEX* and *REFINE* procedures of the *SADONL* software [the 'small molecule' on-line version of *MADNES* (Pflugrath & Messerschmitt, 1991)] using 50 reflections taken from both regions. Accurate values of DET (= 40.325 mm) and θ_D (= -17.951°) were also determined, along with improved cell dimensions, by refinement using 96 and 101 reflections for AC and AD, respectively, from the two regions.

Unit-cell refinement was subsequently performed at ω intervals of 15° during data collection. Crystal data together with some details of structure refinement are given in Table 1. Intensity data corresponding to slightly more than one hemisphere of reciprocal space were recorded using two ω-scan ranges of 100° with a φ shift of 90°(to achieve > 180° in total) at χ = 0°, followed by two ω rotations of 70°, with a φ shift of 90° at χ = 90°, to record the missing cusp data. Throughout the data collection the parameters for the ω increment and measuring time for each frame were 0.15° and 15 s respectively. Data processing included corrections for Lp effects and area detector specific factors, but no correction for absorption. Several extinction reflections were omitted from the refinements for both data sets.

Table 1. *Crystal data and refinements*

	AC	AD
Formula	$C_{24}H_{20}N_2O_4$	$C_{24}H_{18}N_2O_4Cl_2$
Crystal dimensions (mm)	Rod, 0.4 × 0.2 × 0.1	Needle, 0.5 × 0.1 × 0.1
hkl ranges	-12, 12; -15, 15; 0, 16	-11, 11; 0, 13; 0, 38
θ range (°)	0–33.035	0–31.05
Refined mosaic spread (°)	0.625	0.548
Data-collection time (h)	18	18
Maximum (shift/e.s.d.)	0.633 (for x of H43)	0.334 (for z of H4)
No. of measured reflections	8330	13226
No. of unique reflections	5551	5677
No. of unique $F \geq 6\sigma(F_o)$	3652	3718
No. of refined parameters	338	361
R	0.066	0.066
wR	0.081	0.072
Weighting scheme	$w = k[\sigma^2(F_o) + gF_o^2]^{-1}$	
k, g	0.3106, 0.002	2.1375, 0.0002
Residual density (e Å^{-3})		
Minimum	-0.30	-0.39
Maximum	0.39	0.70

The centrosymmetric structures were solved by direct methods using *SHELXS*86 (Sheldrick, 1986) and refined with *SHELX*80 (Sheldrick, 1980) employing full-matrix least squares on F. All non-H atoms were refined anisotropically and H atoms isotropically. H-atom positions were refined following their initial location in a Fourier difference map. Table 1 summarizes crystal data and various details of the structure refinement. Geometrical calculations were carried out with the program *PARST* (Nardelli, 1983), and figures were drawn with *SNOOPI* (Davies, 1980) and *PLUTO*78 (Motherwell & Clegg, 1978).

Analysis of the experimental structures

The molecular structures of AC and AD together with the atom-numbering schemes are shown in Fig. 1. The final atomic coordinates and equivalent U values are listed in Table 2.* Some geometrical parameters relevant to the intercomparison of AC, AD and DPH [the DPH structure is taken from Camerman & Camerman (1971)] are collected together in Table 3.

The hydantoin ring in all three structures is approximately planar. The maximum deviation of a ring atom from the plane is 0.042 (2), 0.053 (3) and 0.03 Å for AC, AD and DPH, respectively, with O atoms at the following distances from the mean plane: O1 -0.092 (2), -0.101 (2), -0.05 Å and O2 0.052 (2), 0.088 (2), 0.09 Å for AC, AD and DPH compounds, respectively. Although both N atoms are substituted in AC and AD the hydantoin bond lengths are the same for all three compounds within the 3σ limit; only N1—C2 of AD

* Lists of structure factors, anisotropic thermal parameters, fractional coordinates, and bond lengths and angles have been deposited with the British Library Document Supply Centre as Supplementary Publication No. SUP 71328 (19 pp.). Copies may be obtained through The Technical Editor, International Union of Crystallography, 5 Abbey Square, Chester CH1 2HU, England.

is slightly longer beyond this limit. The goodness-of-fit parameters for seven hydantoin molecules and two phenyl C atoms, C11 and C21, of AC and AD to the equivalent atoms in DPH are 0.099 and 0.068 Å, respectively. In all three structures, the two phenyl rings attached to C5 are planar within 3σ.

The angles between the least-squares planes and other geometrical parameters thought to be decisive (Camerman & Camerman, 1974) for anticonvulsant activity are given in Table 3. In both AC and AD, carboxylic groups act as proton donors in hydrogen bonds to carbonyl O atoms in adjacent molecules, forming dimers as shown in the packing diagrams, Fig. 2. Some details pertaining to the hydrogen bonding are presented in Table 4. There are no other intermolecular contacts which are shorter than the sum of the appropriate van der Waals radii.

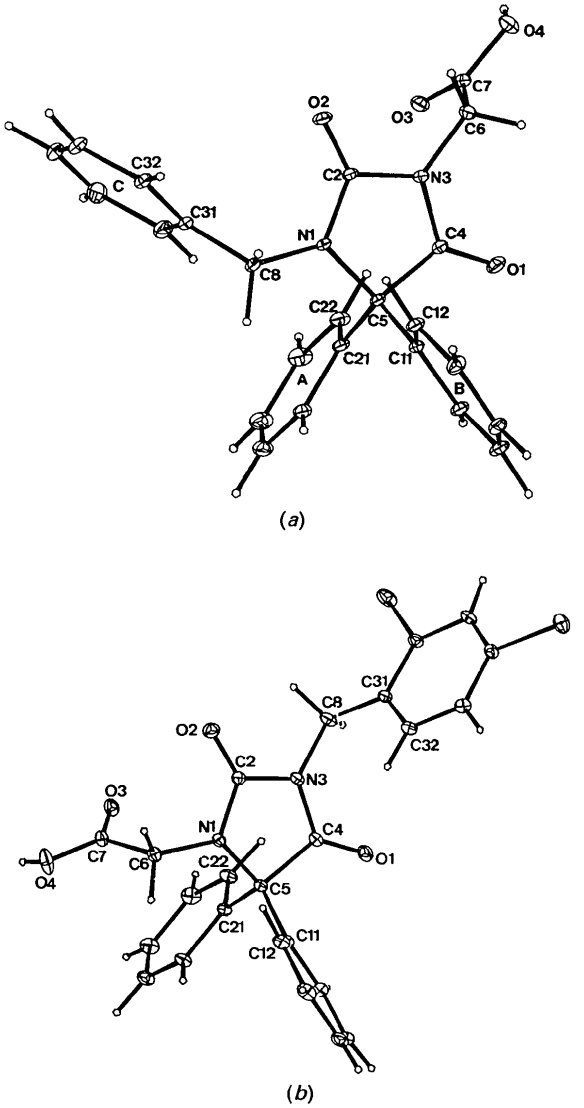

Fig. 1. (*a*) AC and (*b*) AD with atom-numbering scheme. Thermal-vibration ellipsoids enclose 20% probability. *A* and *B* are the centroids of phenyls. Ring *B* is defined as the ring coming out of plane of the paper when the hydantoin is oriented as shown.

Table 2. *Fractional atomic coordinates and equivalent isotropic displacement parameters* (Å^2), *with e.s.d.'s in parentheses*

The form of the displacement factor was $\exp(-2\pi^2\sum_i\sum_j U_{ij}h_ih_ja_i^*a_j^*)$.

$U_{eq} = (U_{11} + U_{22} + U_{33})/3$.

	x	y	z	U_{eq}
AC				
N1	0.3840 (2)	0.6199 (1)	0.1671 (1)	0.0310 (4)
N3	0.6096 (2)	0.7949 (2)	0.2006 (1)	0.0342 (4)
O1	0.5123 (2)	0.9634 (1)	0.2480 (2)	0.0511 (5)
O2	0.6291 (2)	0.5886 (1)	0.1517 (1)	0.0429 (5)
O3	0.8088 (2)	0.9028 (2)	0.4280 (1)	0.0481 (4)
O4	1.0220 (2)	0.9992 (2)	0.3438 (1)	0.0579 (5)
C2	0.5462 (2)	0.6566 (2)	0.1708 (2)	0.0306 (5)
C4	0.4913 (2)	0.8480 (2)	0.2182 (2)	0.0342 (4)
C5	0.3264 (2)	0.7316 (2)	0.1860 (2)	0.0299 (5)
C6	0.7801 (2)	0.8707 (2)	0.2104 (2)	0.0412 (5)
C7	0.8716 (2)	0.9262 (2)	0.3402 (2)	0.0366 (5)
C8	0.2752 (2)	0.4813 (2)	0.1301 (2)	0.0351 (5)
C11	0.2384 (2)	0.7418 (2)	0.0672 (2)	0.0306 (5)
C12	0.2533 (2)	0.6759 (2)	−0.0468 (2)	0.0394 (5)
C13	0.1834 (3)	0.6956 (2)	−0.1534 (2)	0.0494 (6)
C14	0.0988 (3)	0.7803 (2)	−0.1466 (2)	0.0496 (6)
C15	0.0842 (3)	0.8465 (2)	−0.0341 (2)	0.0493 (6)
C16	0.1549 (2)	0.8292 (2)	0.0733 (2)	0.0403 (5)
C21	0.2303 (2)	0.7310 (2)	0.2911 (2)	0.0338 (5)
C22	0.3107 (3)	0.7897 (2)	0.4117 (2)	0.0472 (6)
C23	0.2247 (3)	0.7782 (3)	0.5081 (2)	0.0614 (6)
C24	0.0586 (3)	0.7082 (3)	0.4846 (2)	0.0619 (7)
C25	−0.0239 (3)	0.6513 (2)	0.3648 (2)	0.0514 (6)
C26	0.0611 (2)	0.6627 (2)	0.2686 (2)	0.0398 (5)
C31	0.3166 (2)	0.3990 (2)	0.2095 (2)	0.0353 (5)
C32	0.3499 (3)	0.2889 (2)	0.1542 (2)	0.0489 (6)
C33	0.3802 (3)	0.2065 (3)	0.2222 (3)	0.0690 (6)
C34	0.3774 (3)	0.2333 (3)	0.3441 (3)	0.0707 (6)
C35	0.3468 (3)	0.3433 (3)	0.4021 (3)	0.0752 (7)
C36	0.3152 (3)	0.4267 (3)	0.3327 (2)	0.0552 (6)
AD				
N1	0.2618 (3)	−0.3237 (2)	0.1251 (1)	0.0310 (8)
N3	0.4972 (3)	−0.2135 (2)	0.1133 (1)	0.0356 (8)
O1	0.6920 (3)	−0.3545 (2)	0.1533 (1)	0.0480 (8)
O2	0.2471 (3)	−0.1214 (2)	0.0808 (1)	0.0471 (8)
O3	0.1508 (3)	−0.4150 (2)	0.0311 (1)	0.0454 (8)
O4	−0.0944 (3)	−0.4735 (4)	0.0577 (1)	0.0723 (12)
C2	0.3254 (4)	−0.2105 (3)	0.1035 (1)	0.0338 (9)
C4	0.5509 (4)	−0.3286 (3)	0.1393 (1)	0.0340 (10)
C5	0.3946 (4)	−0.4185 (3)	0.1453 (1)	0.0292 (9)
C6	0.0905 (4)	−0.3620 (3)	0.1145 (1)	0.0369 (11)
C7	0.0523 (4)	−0.4197 (3)	0.0630 (1)	0.0385 (10)
C8	0.6079 (5)	−0.1196 (3)	0.0894 (1)	0.0419 (12)
C11	0.3799 (4)	−0.4521 (3)	0.1999 (1)	0.0315 (8)
C12	0.2707 (5)	−0.3833 (3)	0.2281 (1)	0.0416 (12)
C13	0.2618 (5)	−0.4165 (4)	0.2781 (1)	0.0500 (13)
C14	0.3653 (5)	−0.5146 (4)	0.2997 (1)	0.0524 (14)
C15	0.4756 (5)	−0.5821 (4)	0.2718 (1)	0.0480 (12)
C16	0.4828 (4)	−0.5522 (3)	0.2222 (1)	0.0387 (11)
C21	0.3992 (4)	−0.5476 (3)	0.1129 (1)	0.0318 (9)
C22	0.4991 (4)	−0.5546 (3)	0.0730 (1)	0.0407 (11)
C23	0.4908 (5)	−0.6675 (4)	0.0418 (1)	0.0506 (13)
C24	0.3832 (5)	−0.7736 (4)	0.0494 (1)	0.0521 (13)
C25	0.2848 (5)	−0.7676 (3)	0.0891 (1)	0.0468 (12)
C26	0.2922 (4)	−0.6560 (3)	0.1204 (1)	0.0385 (10)
C31	0.6768 (4)	−0.0018 (3)	0.1209 (1)	0.0341 (10)
C32	0.6446 (4)	0.0170 (3)	0.1700 (1)	0.0378 (10)
C33	0.7140 (4)	0.1247 (3)	0.1978 (1)	0.0403 (11)
C34	0.8159 (4)	0.2155 (3)	0.1755 (1)	0.0377 (10)
C35	0.8484 (4)	0.2035 (3)	0.1268 (1)	0.0416 (11)
C36	0.7806 (4)	0.0937 (3)	0.0996 (1)	0.0373 (10)
Cl1	0.9128 (1)	0.3485 (1)	0.2102 (1)	0.0551 (3)
Cl2	0.8230 (1)	0.0778 (1)	0.0381 (1)	0.0621 (4)

Widespread research (Camerman & Camerman, 1971, 1977; Codding, Duke, Dargie & Benedictson, 1986; Codding, Lee & Richardson, 1984; Jones & Kennard, 1978) on anticonvulsant drugs has led to a model (Wong,

Table 3. *Geometrical parameters for AC, AD and DPH*

	AC	AD	DPH
Selected distances (Å)			
O1—C4	1.202 (2)	1.196 (6)	1.223 (8)
O2—C2	1.211 (2)	1.210 (6)	1.209 (8)
C4—N3	1.361 (2)	1.373 (6)	1.343 (8)
C2—N3	1.404 (2)	1.387 (7)	1.392 (8)
N3—C4	1.361 (2)	1.373 (6)	1.343 (8)
C4—C5	1.540 (3)	1.549 (8)	1.548 (8)
C5—N1	1.470 (2)	1.483 (6)	1.460 (8)
N1—C2	1.338 (2)	1.362 (6)	1.333 (8)
C5—C11	1.530 (3)	1.522 (7)	1.520 (15)
O1···O2	4.564 (2)	4.551 (3)	4.555
O1···*A*	4.161 (2)	4.221 (2)	4.23
O1···*B*	3.922 (3)	3.995 (3)	3.97
O2···*A*	5.657 (3)	5.375 (2)	5.51
O2···*B*	5.514 (3)	5.793 (3)	5.68
A···*B*	4.983 (2)	4.886 (2)	4.84
Selected angles (°)			
Between planes			
Ring *A*—ring *B*	111.6 (7)	73.5 (1)	90.0
Hydantoin—ring *A*	75.8 (9)	77.9 (1)	66.0
Hydantoin—ring *B*	98.8 (8)	63.9 (1)	67.0
Dihedral angles			
C4—C5—C11—C12	92.2 (2)	101.3 (3)	180.0
N1—C5—C21—C22	85.5 (2)	90.5 (3)	−176.7
Bond angle			
C11—C5—C21	114.7 (2)	112.6 (4)	112.5

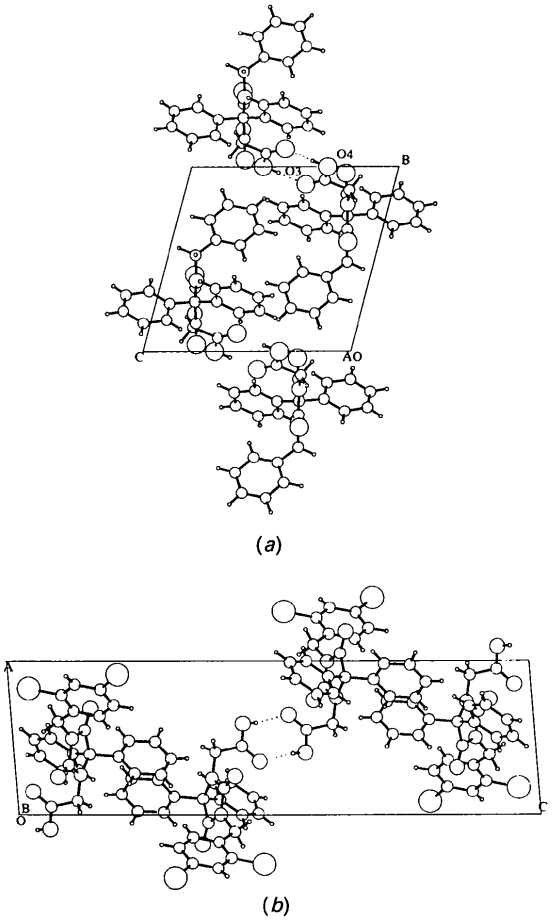

Fig. 2. Packing of the molecules in (010) projection: (*a*) AC, (*b*) AD.

Table 4. *Hydrogen-bonding parameters for AC and AD*

	O4···O3 (Å)	Symmetry operation for O(3)	O4—H4 (Å)	O3···H4 (Å)	O4—H4···O3 (°)
AC	2.664 (2)	$-x+2, -y+2, -z+1$	0.919 (6)	1.758 (1)	168.5 (8)
AD	2.638 (4)	$-x, -1-y, -z$	0.808 (6)	1.86 (4)	160.5 (7)

Defina & Andrews, 1986) still open to debate, which requires one phenyl ring, another hydrophobic region and at least one heteroatom to be present in a specific spatial arrangement for activity. The Camerman & Camerman (1974) model also stresses the importance of stereochemical similarities in the three-dimensional structures of anticonvulsants. Specifically, if the hydrophobic groups of two potential anticonvulsants are spatially superposed, the two electron-donating heteroatoms required in the model should occupy similar regions in space. The data presented in Table 3 show that both active AC and inactive AD have the four potential sites of interaction with the receptor required by the model, in a very similar spatial arrangement to DPH. Those sites are: the two carbonyl O atoms and the phenyl centroids (*A* and *B*).

The obvious difference between the two structures studied here is that the substituents at two N atoms swap places. The imide N atom N3 of inactive AD is blocked by dichlorobenzyl; in active AC, this N atom is bonded to an acetyl group capable of forming hydrogen bonds. Indeed, such bonds are present in the crystal structure (Fig. 2). The importance of an imide N atom acting as a proton donor in the interaction with the receptor was stressed by Codding *et al.* (1986). However, this condition is not considered as *sine qua non* in either of the two models discussed.

A further effect to consider is that the acetyl group in AD may interact with one of the phenyls. The distance between the centre *A* of the phenyl and one of the carboxyl O atoms O3 is 3.302 (2) Å, the angle *A*—C7—O3 is 94.4 (2)° and the angle between C7—O3 line and the phenyl plane is 2.7(2)°. It follows that O3 is positioned below the centre of the ring. The plane of the carboxylate group (defined by O4—C7—O3) is inclined at an angle of 35° to the phenyl plane, whereas a parallel arrangement would be expected from a simple electrostatic argument. So the observed orientation of the carboxylate group may be due to a stereoelectronic interaction with the phenyl, which in turn could disfavour the recognition of the receptor active site, leading to a lack of anticonvulsant activity. This hypothesis is consistent with the models discussed above, in that two hydrophobic regions must be available for the interaction with the receptor.

Computation

The analysis of the molecular conformation found in the crystal structure offers some explanation for the differing

pharmacological activity of AC and AD. However, there are obvious dangers in making such an interpretation based only on the crystal structure. The carboxylate group in AD may be held in such an orientation because of hydrogen bonding (which *is* present in the crystal) from neighbouring molecules. There may also be some more subtle steric effect which means that this molecular conformation is favoured.

We can attempt to answer these last two points by carrying out molecular mechanics calculations, using a model force field which is free from intermolecular interactions. At the same time we should be cautious in interpreting these results, since (i) the free molecule is not necessarily a better model for the situation found in solution, and (ii) if there are stereoelectronic effects, the force field may not properly take these into account. Because of these problems, it is vital to supplement such molecular mechanics results with *ab initio* calculations, which can give some clue as to whether intramolecular interactions are important. Furthermore, looking for similarities and differences in electronic structure between AC, AD and DPH may give us new insight into the different activity of these molecules, perhaps by showing that some feature of the electron distribution (the density in a lone pair, for example) is measurably perturbed in AD in a way which does not occur in AC and DPH.

Molecular mechanics

The substituent groups at N1 and N3 in AC and AD may change their torsional angles in solution, depending on the barrier height to rotation. Therefore it was worthwhile to see whether substantially different conformations might be energetically favourable for isolated molecules, using molecular mechanics (MM). The MM calculations also have the useful effect of idealizing the geometries of the three molecules in preparation for the MO calculations - a necessary step, because (for example) the H atoms in this study and in the Camerman & Camerman study of DPH were treated differently.

MM calculations were carried out with *CHEMX* (Davies, 1991) in two stages: (i) a potential surface scan with respect to torsional angles, followed by (ii) minimization starting from the 15 lowest energy structures found in (i). An electrostatic interaction was incorporated into the force field, within the usual point-charge approximation. To this end, the *MINDO*3 semi-empirical option of *GAUSSIAN*90 (Frisch *et al.*, 1990) was used to generate population analysis charges, based on the in-crystal conformations. Two other options were also tried for one molecule (DPH): 'Gasteiger' charges (Gasteiger & Marsili, 1980) and no charges. Some significant differences were found between the three predicted minimum-energy structures (steepest descent minimization from the crystallographic structures), but no one choice gave conspicuously better agreement with the experimental (crystallographic) conformations.

DPH has only two (phenyl) torsional angles to be considered, whereas AC and AD both have six. In all the molecules, the two phenyl torsional angles (τ_1 = C4—C5—C11—C12, τ_2 = C4—C5—C21—C22) were varied. In AD, two additional angles associated with the $-CH_2-CO_2H$ group (τ_3 = C2—N1—C6—C7, τ_4 = N1—C6—C7—O3) were varied, since these are implicated in the model for pharmacological activity. In AC, the extra two angles varied were those of the benzyl group (τ_5 = C2—N1—C8—C31, τ_6 = N1—C8—C31—C32) for essentially the same reason. The bond rotations were carried out in 30° steps, with phenyl rings rotated through a total of 180° and other bonds through 360°, generating the following total number of conformations: AD (7056); AC (2592); DPH (144). The three lowest energy structures from (ii) were then used in single-point *ab initio* calculations with CEP-4G and STO-3G basis sets, using *GAUSSIAN*90.

Fig. 3 shows the ten lowest energy structures superimposed for each molecule. Of these ten, the differences in energy between the lowest and the highest energy structures are: 0.05 (AD), 0.04 (AC), 0.04 eV (DPH) per molecule. This is only about twice the amount of thermal energy available at room temperature (kT = 0.025 eV) for interconversion between the structures (although there may be sizeable barriers between different local minima). In DPH, there is evidently significant rotation of the phenyl groups, whereas AC and AD show more restricted rotation, probably as a result of interaction with the substituent groups.

In AD, the ten lowest energy conformations contain a wide range of angles τ_3 and τ_4, although in eight of the ten (including the lowest one) these angles are within 25° of each other, and the phenyl-carbonyl distance is greater than 4 Å, in contrast to the crystal structure result of 3.3 Å. The in-crystal value of τ_3 is 72.1(4)°, and this changes to 92° in the lowest energy structure. τ_4 changes greatly in going from the crystal structure to the minimum one, from -10.5(4) to +179°. The most likely explanation for this difference is that an intermolecular hydrogen bond restricts the motion of this group in the crystal structure.

In AC, the ten lowest energy structures fall into four groups with similar values of τ_5 and τ_6, the largest containing four structures (including that with the lowest energy). The four groups correspond to quite distinct conformations, and since they are all within 0.04 eV, there is probably no well defined global minimum-energy structure at room temperature.

Pseudopotential calculations

The effective core potentials (ECP's) of Stevens, Basch & Krauss (1984) were chosen for the computation of DD's, in combination with the STO-4G basis set developed by those authors. This was shown to give good agreement with all-electron calculations for conforma-

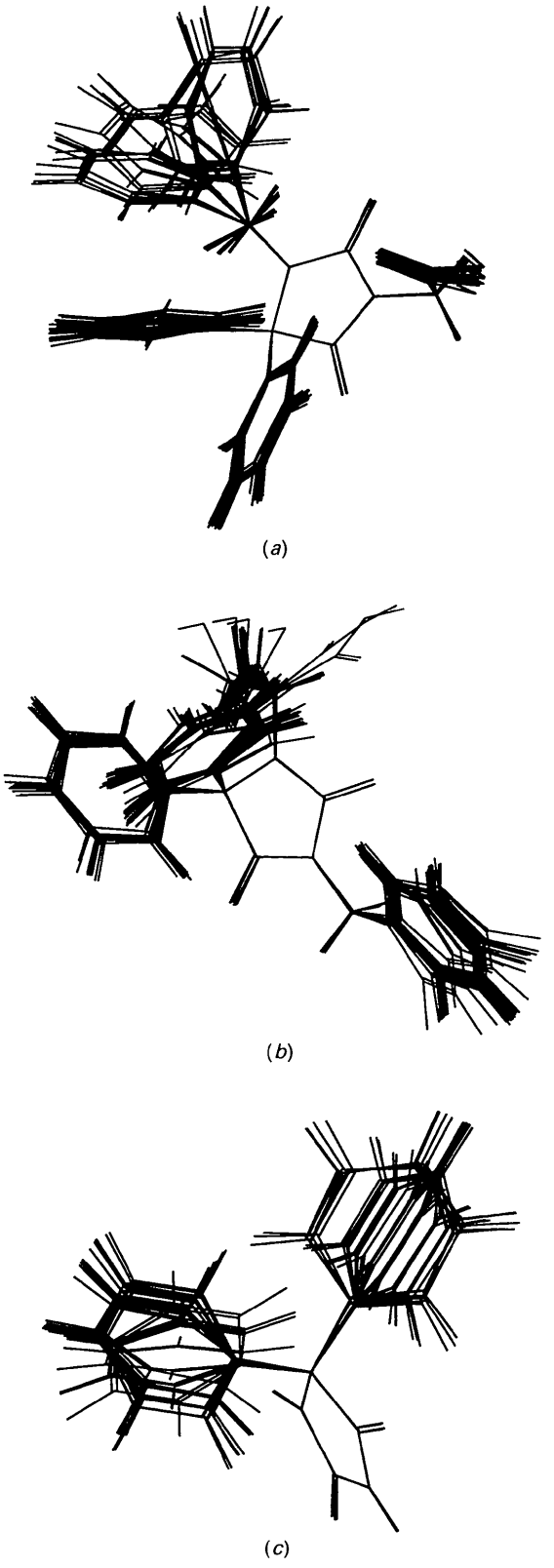

Fig. 3. The ten lowest energy (MM force field) structures superposed for (*a*) AC, (*b*) AD and (*c*) DPH.

tions and properties such as dipole moments. The DD reflects changes which occur in the valence-electron distribution of atoms when they form chemical bonds, so the pseudopotential approximation is not a severe one for this purpose. Most experimentally determined DD's [for example those generated with the popular multipole model of Hansen & Coppens (1978)] also ignore core polarization effects.

Figs. 4(*a*)-4(*c*) are DD maps computed with *FSTRUCT* (Howard, 1991) in the plane of the hydantoin ring. To obtain the DD, the density from a 'promolecule' was subtracted from the total density. The promolecule was defined in the usual way: as the summed free-atom densities computed with the same basis set and repopulated to give spherically symmetric atoms. The valence density at the N-atom positions in AC and AD closely resembles that in DPH, despite the differing substituents. The build up of density in the C4—C5 bond is the most prominent feature on all three maps, with the peak height differing slightly between DPH (0.20 e $Å^{-3}$) and AC and AD (0.25 e $Å^{-3}$). The oxygen lone-pair density also differs little between the three compounds; in particular, the zero contour, a feature sensitive to intermolecular and intramolecular interactions (Eisenstein, 1988), is very similar in all cases.

So these maps suggest little significant perturbation of the oxygen lone-pair density in either AC or DC as a result of adjacent substituents groups, as compared with DPH which just has H atoms bonded to N1 and N3. Deformation maps in the planes of the two phenyl rings attached to C5 also showed no significant differences between the three molecules. Fig. 5(*a*) shows the AC deformation density in a plane cutting through the nearest phenyl ring attached to C5 and the substituent group on N1. The zero contour between these two groups is fairly symmetric. Fig. 5(*b*), an equivalent map for AD, shows a rather more asymmetric zero contour, with the valence shell of C7 possibly showing a slight distortion in the direction of the phenyl ring. This is possibly an indication of an intramolecular interaction.

The CP analysis developed by Bader and co-workers (Bader, 1990) is perhaps a more sensitive probe of electronic structure, and certainly a more quantitative one. The set of CP's in $\rho(\mathbf{r})$, $\mathbf{r}_c$ are defined such that $\nabla\rho(\mathbf{r}_c) = 0$. We shall be concerned with two of the four types of CP which occur: (3, -1) and (3, +1) or 'bond' and 'ring' CP's. The value of ρ_c in a bond measures its strength; the trace of the (diagonalized) Hessian at $\mathbf{r}_c$ measures the extent of depletion or concentration of charge; and the ratio of eigenvalues of this matrix (the bond 'ellipticity' ε) measures the degree of planarity or conjugation. More precisely, $\varepsilon = \lambda_2/\lambda_1 - 1$, where the λ's are the two eigenvalues of the Hessian corresponding to directions perpendicular to the bond.

Stationary points in $\nabla^2\rho$, points of maximum charge concentration or depletion, are utilized in theories of

reactivity (Shi & Boyd, 1991). A (3, -3) CP in $\nabla^2\rho$, a local maximum, occurs in the region of the density associated with a lone pair of electrons. An attempt was made to locate all the BCP's and RCP's with the program *SADDLE* (Laidig, 1989), with only limited success. For example, in the hydantoin ring only two of the five BCP's could be located in all three molecules. This was despite the fact that a visual inspection of the total (valence) density indicates that all BCP's *are* present, although $\rho(\mathbf{r})$ is much flatter than in a corresponding all-electron calculation. This is perhaps slightly surprising, since any meaningfully defined 'core' electron density ought to be negligibly small in the middle of a bond: certainly, the $1s.1s$ core product cannot be appreciable there. But it is evident that core-valence products (absent in the pseudopotential, valence-only density) must be essential to realistically describe the *shape* (*i.e.* curvature) of $\rho(\mathbf{r})$ in a bond, even if the magnitude is well represented. Therefore, these calculations cannot be expected to give meaningful results for the BCP's, even

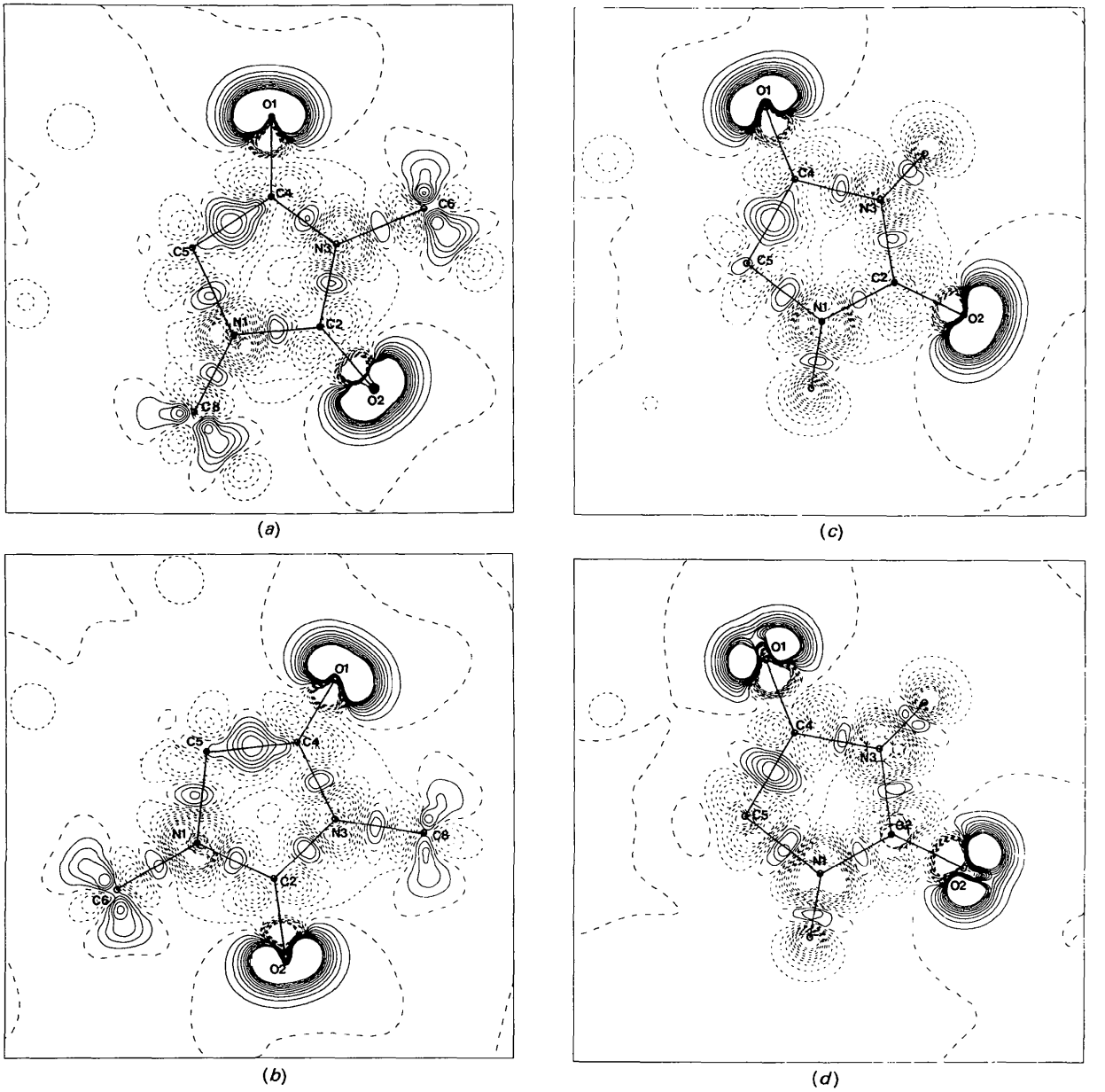

Fig. 4. Theoretical deformation densities of (*a*) AC, (*b*) AD and (*c*) DPH, CEP-4G basis set, and (*d*) DPH, STO-3G basis set: contours at 0.05 e Å^{-3} intervals; negative contours broken.

when they could be located successfully by *SADDLE*. All-electron calculations were therefore necessary in order to carry out the envisaged CP analysis.

All-electron calculations

Minimal basis (STO-3G) wavefunctions were generated for all three compounds. In the case of AD, H atoms were substituted for the two Cl atoms, giving a molecule isoelectronic with AC. As mentioned earlier, the Cl atoms had only been included to improve crystallization and had not altered the pharmacological activity (or lack of it), so this is a reasonable step. The basis set size was increased, therefore, to 170 functions (AC, AD), 108 (DPH), compared with the pseudopotential bases sizes of 140 (AC, AD) and 88 (DPH). Fig. 4(*d*) shows the hydantoin ring STO-3G deformation density. Compared to the CEP-4G result in Fig. 4(*c*) this reveals only very small differences, thus demonstrating the validity of the pseudopotential approximation at least for DD's.

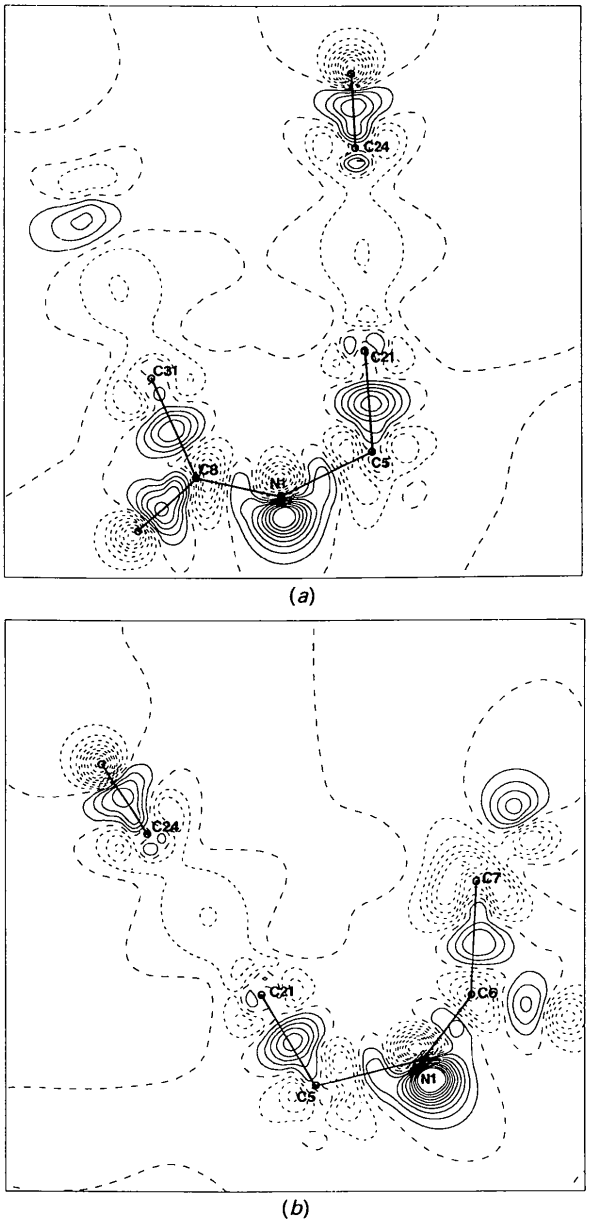

Fig. 5. Theoretical deformation densities of: (*a*) AC in plane containing atoms C21, C24, C31; (*b*) AD in plane containing atoms C21, C24, C7.

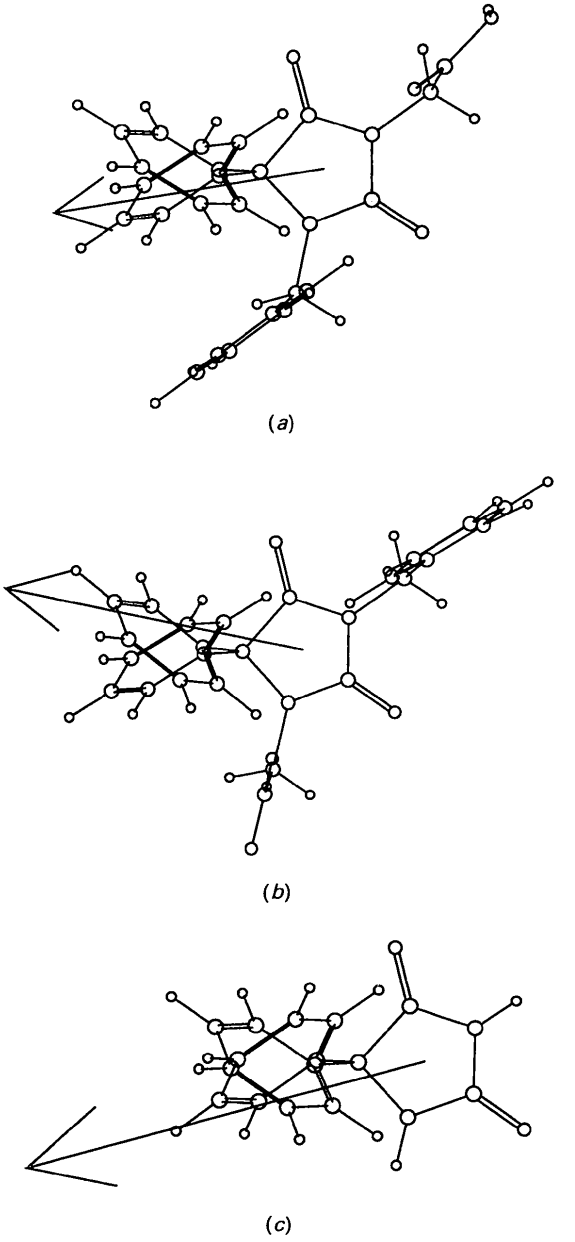

Fig. 6. Orientation of STO-3G dipole moments for (*a*) AC, (*b*) AD and (*c*) DPH.

The STO-3G dipole moment magnitudes in AC, AD and DPH are: 4.6704, 5.3376 and 7.000 × 10^{-30} C m, respectively, and their directions are indicated in Fig. 6. The directions may be compared if the molecules are oriented to make the hydantoin rings as near-coincident as possible, and these are the orientations shown in Fig. 6. The dipole directions are more similar for the two active compounds AC and DPH (the vectors make an angle of 20° for DPH and AC, and approximately 30° for both AC–AD and AD–DPH). This may be linked with the difference in activity - but it is difficult to be certain how much the directions would change if larger basis sets could be employed.

All CP's, including RCP's, could now be located with *SADDLE*. Table 5 reports the values of ρ_c, $\nabla^2\rho_c$ and the ellipticities for the five bonds of the hydantoin ring plus two carbonyl bonds. The only bond in the hydantoin ring which is chemically identical in all three molecules is C4—C5, and the CP properties are indeed nearly identical in DPH, AC and AD. A similar degree of transferability applies to the carbonyl bonds - the high ε reflects the fact that this is formally a double bond. So again, this gives us no basis for distinguishing between the three molecules. The remaining four bonds show more varied behaviour; but there are no clear trends which would indicate closer (electronic) similarity between AC and DPH than between the other two possible pairings of molecules.

The RCP's do indicate a distinction between AD and AC and DPH. The values of ρ_c and $\nabla^2\rho_c$ are closer for DPH and AC than for DPH and AD in the hydantoin ring; but in the two phenyl rings, it is AC and AD which are evidently more similar. The MM calculations indicated that the phenyl groups are least rigid in DPH, which may relate to this difference in electronic structure. Table 7 contains the properties of the oxygen lone pair CP's in $\nabla^2\rho_c$. First, we consider the two carbonyl O atoms O1 and O2 of the hydantoin core, common to all three molecules. The distances from the O-atom nuclei to the lone-pair CP's are 0.3172 (3) for O1—CP and 0.3194 (3) Å for O2—CP in all three molecules. The values of $\rho(\mathbf{r}_c)$ and $|\nabla\rho(\mathbf{r}_c)|$ show

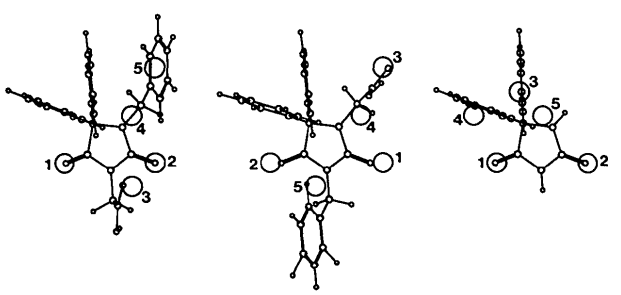

Fig. 7. Positions of the five lowest electrostatic potential minima in AC, AD and DPH, marked by circles. The numbers 1-5 indicate the ordering of the minima, with 1 the lowest.

Table 5. *Ring-critical points*

Ring	ρ_c (e Å^{-3}) DPH	AC	AD	$-\nabla^2\rho_c$ (e Å^{-5}) DPH	AC	AD
Hydantoin	0.351	0.351	0.344	−9.64	−9.62	−9.47
Ph1	0.169	0.169	0.169	−4.05	−3.98	−3.98
Ph2	0.175	0.169	0.169	−4.27	−3.95	−3.95

Table 6. *Bond-critical points*

Bond	ρ_c (e Å^{-3}) DPH	AC	AD	$-\nabla^2\rho_c$ (e Å^{-5}) DPH	AC	AD	ε DPH	AC	AD
C4—C5	1.71	1.71	1.71	16.1	16.1	16.0	0.07	0.06	0.06
C4—N3	1.98	1.98	1.99	−4.96	−3.57	−3.47	0.16	0.16	0.17
N3—C2	2.01	2.00	2.03	−3.01	−1.42	−1.23	0.18	0.17	0.19
C2—N1	1.98	2.03	1.96	3.45	3.59	4.75	0.22	0.23	0.22
N1—C5	1.69	1.69	1.69	6.68	7.47	7.54	0.03	0.03	0.03
C2—O2	2.50	2.50	2.50	−17.9	−17.2	−18.2	0.33	0.31	0.32
C4—O1	2.42	2.42	2.42	−24.3	−23.8	−24.0	0.36	0.35	0.36

Table 7. *Oxygen lone pair* (3, −3) *critical points in* $\nabla^2\rho$

	ρ_c (e Å^{-3}) DPH	AC	AD	$\nabla\rho_c$ (e Å^{-4}) DPH	AC	AD	$-\nabla^2\rho_c$ (e Å^{-5}) DPH	AC	AD
O1*a*	7.693	7.686	7.680	20.80	20.80	20.77	201.0	200.5	200.0
O1*b*	7.713	7.707	7.707	20.82	20.81	20.81	202.4	201.9	201.7
O2*a*	7.605	7.578	7.592	20.56	20.49	20.52	193.0	190.6	192.1
O2*b*	7.599	7.585	7.585	20.54	20.49	20.51	192.5	191.1	191.3
O3*a*	..	7.689	7.672	..	20.80	20.76	..	200.0	198.6
O3*b*	.	7.719	7.711	.	20.85	20.82	.	202.1	201.3
O4*a*	..	7.677	7.671	..	20.63	20.60	.	197.3	197.1
O4*b*	.	7.654	7.647	.	20.60	20.58	.	195.9	195.5

very little variation. The $\nabla^2\rho(\mathbf{r}_c)$ values indicate O2 substituent intramolecular interactions in both AC and AD, not present in DPH (the O1 values are more similar for all three molecules). However, the differences are very small, and the pattern of the interaction is not consistent with the idea that the oxygen lone pairs are perturbed in (inactive) AD in a way that distinguishes it from (active) AC and DPH.

The remaining data in Table 7 refer to the carboxyl O atoms O3 and O4, present in the acetyl group of AC and AD. Differences between the Laplacian critical-point properties for these two groups must be attributed to differing intramolecular interactions. However, even the values of $\nabla^2\rho(\mathbf{r}_c)$ are almost identical for the two acetyl groups, the biggest difference occurring for the lone pair O3*a* which shows a change of less than 1%. The size of the differences is roughly the same as found for O1 and O2, indicating that intramolecular effects are no stronger for the acetyl fragment than these ring atoms. It should be recalled that these CP's are located where $\nabla^3\rho(\mathbf{r}_c) = 0$, so their position and the values of properties there should be very sensitive to a perturbation in the shell structure of an atom.

In Fig. 7 we compare the positions of local minima in the electrostatic potential (EP), generated within a point-charge approximation, using the population analysis charges from the STO-3G calculations (an inspection of the EP's drawn as three-dimensional iso-contours did not reveal anything useful). Not surprisingly, the two lowest are in the vicinity of the oxygen lone pairs for all three molecules. The position of the minima

differs slightly between (inactive) AD and (active) AC and DPH: in the former, the minimum is closer to the lone-pair positions. It should be noted that this is not due to a change in the lone-pair positions in AC, since only charges centred on the nuclei are used in computing these maps (no explicit lone-pair charges are used). Rather it must be the result of the different environment of the lone-pair electrons, because of the vicinity of substituents. In DPH the next two lowest EP local minima are associated with the biphenyl group, whereas the next lowest minimum in AC and AD occurs near the carbonyl O-atom substituent.

Concluding remarks

An analysis of molecular geometries derived from an X-ray crystal structure determination suggested an explanation for the inactivity of AD. The molecular mechanics calculations have indicated that the conformation of the free molecule may be considerably different, because of the absence of intermolecular hydrogen bonds. However, it should be stressed that hydrogen bonding to the receptor is likely to occur, so that the free molecule geometry is not necessarily more 'realistic' than the in-crystal one.

To be sure, the minimal basis-set calculations presented here will give values for ρ, $\nabla^2\rho$ *etc.* or the DD at some point which will be significantly different from their Hartree-Fock limit values. But only relative trends are being compared here, no significance is attached to the absolute values. It is quite possible that even the trends might change if bigger basis sets could be used, especially if diffuse functions were present on the O atoms, and this is still under investigation.

The electronic structure comparisons gave some results which may be linked to differences in pharmacological activity. One of the simplest indicators, the dipole moment direction, indicated an electronic dissimilarity between AD and AC and DPH, as did the positions of local minima in the EP and the hydantoin RCP $\nabla^2\rho$ values.

Little attention has been paid previously to the electron density in the hydantoin ring as an indicator of anticonvulsant activity. It has been demonstrated that both deformation maps and $\nabla^2\rho$, particularly in the region of lone-pair CP's, can be used to detect and (in the case of $\nabla^2\rho$) quantify intramolecular interactions between substituent groups or atoms, although the effects are evidently small in these molecules. More work is clearly needed in this area to see if these can be decisive indicators of activity; but the results presented here contain some promise of this.

These MO calculations have looked for intrinsic similarities/differences between 'isolated' drug molecules, without considering the influence of a receptor, or of solvent molecules. The explicit inclusion of water molecules during minimization would provide a way of modelling the latter. Some crude model of the drug molecule-receptor interaction is not beyond the bounds of computational feasibility. For example, computing the molecular polarizability tensor might reveal similarities in the induced dipole interaction between a molecule and a receptor. Since the degree of polarization might be large, it might be more useful to study the effect of applying a realistically sized field rather than the polarizability tensor itself. A 'charge sensitivity analysis', which explores the response of a molecule to external perturbations *via* atoms-in-molecules representations of softness and hardness tensors (Nalewajski & Korchowiec, 1989) provides an alternative approach.

We are very grateful to British Council for a grant enabling us to carry on this research, and to the Polish State Committee for Scientific Research (KBN) for sponsoring the work under project No. 2 2612 92 03. Dr P. A. Borea of the Institute di Farmacologia, Universite di Ferrara, is gratefully acknowledged for supplying the results of receptor binding experiments. Dr C. W. Lehmann gave some assistance with *CHEMX*.

References

ALDRICH, H. S. & KIER, L. B. (1974). *Molecular and Quantum Pharmacology*, edited by E. BERGMANN & B. PULLMAN, pp. 229-240. Dordrecht: D. Reidel.

ANDREWS, P. R. (1969). *J. Med. Chem.* **12**, 761.

ANDREWS, P. R. & WONG, M. G. (1989). *Eur. J. Med. Chem.* **24**, 323-334.

BADER, R. F. (1990). *Atoms in Molecules – a Quantum Theory*. International Series of Monographs in Chemistry 22. Oxford Univ. Press.

BOREA, P. A. (1991). Private communication.

BROUILLETTE, W. J., BROWN, G. B., DELOREY, T. M. & LIANG, G. (1990). *J. Pharm. Sci.* **79**, 871-874.

CAMERMAN, A. & CAMERMAN, N. (1971). *Acta Cryst.* **27**, 2205-2211.

CAMERMAN, A. & CAMERMAN, N. (1974). *Molecular and Quantum Pharmacology*, Vol. 4, edited by E. BERGMANN & B. PULLMAN, pp. 213-227. Berlin: D. Reidel.

CAMERMAN, A. & CAMERMAN, N. (1977). *Proc. Natl Acad. Sci. USA*, **74**, 1264-1266.

CODDING, P. W., DUKE, N. E., DARGIE, R. L. & BENEDICTSON, M. S. (1986). In *Proceedings of Sixth Symposium on Organic Crystal Chemistry,* Poznań-Rydzyna, Poland.

CODDING, P. W., LEE, T. A., RICHARDSON, J. F. (1984). *J. Med. Chem.* **27**, 649-654.

DAVIES, E. K. (1980). *SNOOPI*. Chemical Crystallography Laboratory, Univ. of Oxford, England.

DAVIES, E. K. (1991). *CHEMX*. Chemical Design Ltd, Oxford, England.

EISENSTEIN, M. (1988). *Acta Cryst.* B**44**, 412-426.

FRISCH, M. J., HEAD-GORDON, M., TRUCKS, G. W., FORESMAN, J. B., SCHLEGEL, H. B., RAGHAVACHARI, K., ROBB, M., BINKLEY, J. S., GONZALEZ, C., DEFREES, D. J., FOX, D. J., WHITESIDE, R. A., SEEGER, R., MELIUS, C. F., BAKER, J., MARTIN, R. L., KAHN, L. R., STEWART, J. J. P., TOPIOL, S. & POPLE, J. A. (1990). *GAUSSIAN*90. Revision F. Gaussian Inc., Pittsburgh, USA.

GASTEIGER, J. & MARSILI, M. (1980). *Tetrahedron*, **36**, 3219-3228.

HANSEN, N. K. & COPPENS, P. (1978). *Acta Cryst.* A**34**, 909-921.

HOWARD, S. T. (1991). *FSTRUCT. An Ab Initio One-Electron Properties Program*. Unpublished.

JEFFREY, G. A. & PINIELLA, J. F (1991). Editors. *The Application of Charge Density Research to Chemistry and Drug Design*. New York: Plenum Press.

JONES, P. G. & KENNARD, O. (1978). *J. Pharm. Pharmacol.* **30**, 815-817.

KIĘC-KONONOWICZ, K., ZEJC, A. & KOLASA, K. (1989). *Abstracts of a Polish Pharmaceutical Society Meeting at Wroclaw*, Vol. 8, p. 60.
LAIDIG, K. E. (1989). *SADDLE* and *SADD2R. Part of the PROAIM PROperties of Atoms in Molecules Package*. McMasters Univ., Ontario, Canada.
MOTHERWELL, W. D. S. & CLEGG, W. (1978). *PLUTO78. Program for Plotting Molecular and Crystal Structures*. Univ. of Cambridge, England.
NALEWAJSKI, R. F. & KORCHOWIEC, J. (1989). *J. Mol. Catal.* **54**, 324-342.
NARDELLI, M. (1983). *Comput. Chem.* **7**, 95-98.
PFLUGRATH, J. & MESSERSCHMITT, A. (1991). *MADNES*. Small molecule version. Enraf-Nonius, Delft, The Netherlands.
RUEDENBERG, K. & SCHWARZ, W. H. E. (1990). *J. Chem. Phys.* **92**, 4956-4969.
SCROCCO, E. & TOMASI, J. (1978). *Adv. Quantum Chem.* **11**, 116-190.
SHELDRICK, G. M. (1980). *SHELX80. Program for Crystal Structure Determination*. Univs. of Cambridge, England, and Göttingen, Germany.
SHELDRICK, G.M. (1986). *SHELXS86. Program for Crystal Structure Solution*. Univ. of Göttingen, Germany.
SHI, Z. & BOYD, R. J. (1991). *J. Phys. Chem.* **95**, 4698-4701.
STEVENS, W. J., BASCH, H. & KRAUSS, M. (1984). *J. Chem. Phys.* **81**, 6026-6033.
STONE, A. J. (1981). *Chem. Phys. Lett.* **83**, 233-239.
WONG, M. G., DEFINA, J. A. & ANDREWS, P. R. (1986). *J. Med. Chem.* **29**, 562-572.
ZEJC, A., KIEĆ-KONONOWICZ, K., CHLON, G., KLEINROK, Z., KOLASA, K., PIETRASIEWICZ, T. & CZECHOWSKA, G. (1989). *Pol. J. Pharmacol. Pharm.* **41**, 483-493.

Acta Cryst. (1994). B**50**, 96–106

Solids Modelled by Crystal Field *Ab Initio* Methods. 5.* The Phase Transitions in Biphenyl from a Molecular Point of View

BY A. T. H. LENSTRA, C. VAN ALSENOY, K. VERHULST AND H. J. GEISE

University of Antwerp (UIA), Department of Chemistry, Universiteitsplein 1, *B*-2610 *Wilrijk, Belgium*

(*Received* 21 *January* 1992; *accepted* 26 *July* 1993)

Abstract

Using *ab initio* calculations at the 4-21G level and procedures for extrapolation to r_g geometry as well as using the electrostatic crystal field (ECF-MO) approach, the geometry and torsion potential were calculated for 1,1′-biphenyl in the gas phase, in the $P2_1/a$ lattice with $Z = 2$ and in the Pa lattice with $Z = 4$. At all stages excellent agreement is obtained with available diffraction data, including L_{22} librational components between 293 and 40 K. The following molecular picture emerged when the molecule goes from the gas phase through the solid-state phases biphenyl I, biphenyl II and biphenyl III. In the gas phase biphenyl is twisted ($|\varphi| = 45.7°$) with a relatively high torsion barrier [$\Delta E(\varphi) = 7.9$ kJ mol^{-1}], decreasing to $|\varphi| = 27°$ and $\Delta E(\varphi) = 3.0$ kJ mol^{-1} in the $P2_1/a$ lattice of biphenyl I. In $P2_1/a$, each molecule is librating (in dynamical disorder) between an image form ($\varphi = +27°$) and a mirror-image form ($\varphi = -27°$). At 40 K a phase transition to biphenyl II takes place in which half of the molecules freeze into the image and half into the mirror-image enantiomer. They form racemic pairs along the *ab* diagonals of the *Pa* lattice. Since $Z = 4$ in the *Pa* lattice, there are two types of racemic pairs, *viz.* *AA′* and *BB′* with $|\varphi(A)| = 37.7$ and $|\varphi(B)| = 38.9°$. The observed incommensurability along **a*b*** between 17 and 40 K (biphenyl II) is associated with order/disorder competition of *AA′* and *BB′* pairs. The observed incommensurability along **b*** below 17 K (biphenyl III) is associated with the slow disappearance of domain boundaries. These are stacking faults as a result of glide planes left as relics of the original $P2_1/a$ structure. The calculations attribute $\Delta H = 0.33$ kJ mol^{-1} to the transition at 40 K and $\Delta H = 0.17$ kJ mol^{-1} to the transitions through the various incommensurate phases including that at 17 K. The values compare very well with those obtained by calorimetry. The model also rationalizes observations such as the approximate doubling of the *b* axis at 40 K, the quasi-temperature independent long-range order of 0.67 and $|\langle\varphi\rangle| = 10°$ in biphenyl II, as well as the length of the incommensurate wavevector in biphenyl III.

Introduction

Biphenyl (Fig. 1) is known to exhibit a complex conformational behaviour which depends on the aggregation state and the temperature. The purpose of this work is to rationalize the energetical and geometrical phenomena which take place when the molecule goes from the gaseous state through the various solid-state phases, including those that are incommensurate. In his paper on the temperature-dependent torsion potential Busing (1983) has summarized the considerable body of existing literature on this matter, so that here we will mention only those investigations of immediate relevance.

* Part 4: Lenstra, Van Alsenoy, Popelier & Geise (1994).